Ultrasonication affects the bio-accessibility of primary dairy cow manure digestate for secondary post-digestion

Authors:

Matthijs H. Somers[a], Julie Jimenez[b], Samet Azman[a], Jean-Philippe Steyer[b], Jan Baeyens[a,c], Lise Appels[a,1]

[a] KU Leuven, Department of Chemical Engineering, Process and Environmental Technology Lab, Jan Pieter De Nayerlaan 5, B-2860 Sint-Katelijne-Waver, Belgium

[b] INRAE, LBE, Univ Montpellier, 102 Avenue des Etangs, 11100 Narbonne, France

[c] Beijing University of Chemical Technology, Beijing Advanced Innovation Centre for Smart Matter Science and Engineering, Third East Road, 120009, Beijing, China

[1] corresponding author: Lise Appels lise.appels@kuleuven.be

Keywords: fractionation; hydrolysis; dairy cow manure digestate; bio-accessibility; ultrasound

1. Introduction

Anaerobic digestion (AD) is a well-known microbial degradation process of organic matter to generate biogas (55-75% CH_4) and a nutrient-rich digestate [1]. The overall degradation efficiency and rate are limited when complex organic substrates such as mixed organic waste, restaurant and household waste, or manure are used as substrates [2]. The low degradation efficiency is due to the presence of non-biodegradable compounds and low bio-accessibility of the organic matter [3]. A compound is considered "bio-accessible" when accessible for microbial degradation, the latter depending mostly upon both physical characteristics (e.g., particle size and/or its porosity) and biodegradability of the complex molecules within each fraction [4]. Only a part of the bio-accessible fraction is biodegradable by microorganisms [5]. An organic molecule is biodegradable when it is digestible by microorganisms. A low bio-accessibility leads to a low biodegradability and slow hydrolysis, itself considered to be the rate-limiting step of the overall AD process [6]. To counteract this hydrolysis limitation, a substrate pretreatment is currently being widely researched and applied by (*i*) degrading complex organic compounds into more accessible forms, (*ii*) increasing the particle surface area to enhance contact between bacteria and organic matter and (*iii*) improving the biodegradable character of the organic matter [7]. Although the possible formation of inhibitory substances by the pre-treatment can limit its uses [8].

It was recently proposed by many authors that a digestate disintegration prior to a post-digestion step can be a more efficient way to increase the overall hydrolysis and methane production rates [9]. This research can still be considered as a quite new topic in the literature [10]. Digestate disintegration is proposed as more effective than an overall pretreatment [11] which is the current business-as-usual (BAU), since fed substrates generally already contain a considerable amount of readily biodegradable organic matter that can easily be converted during AD [12]. Figure 1 depicts both alternative scenarios of the BAU approach with a substrate pretreatment, and a scenario of a successive first digester of non-pretreated substrate, AD_a, followed by a secondary digestion (post-digestion, AD_b) that treats the digestate of AD_a. This figure is a schematical representation of the envisioned full-scale continuous application of digestate disintegration.

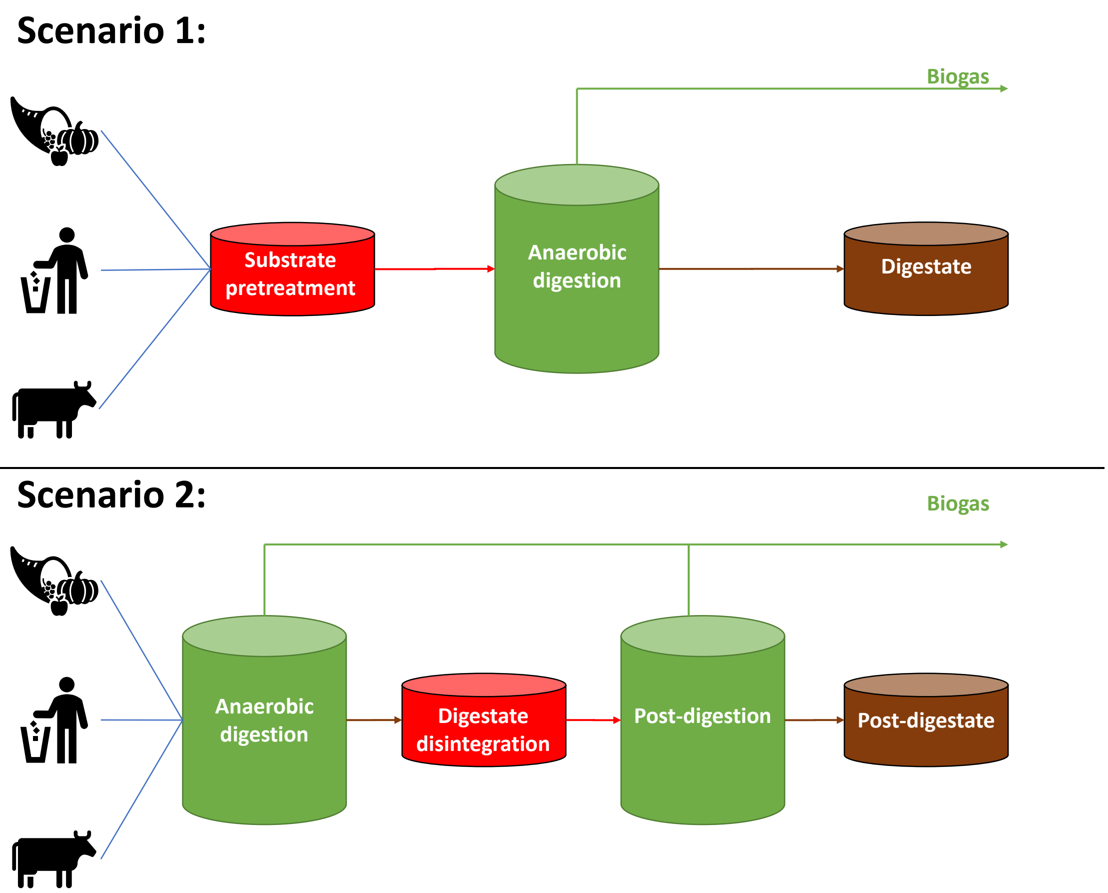

Figure 1: Alternative configurations with overall substrate disintegration in scenario 1, and digestate disintegration and post-digestion in scenario two.

The second scenario's main objective is to enhance the biodegradability of the refractory compounds that are not usually degraded during AD, hence applying a more focused use of energy and/or chemical agents during the digestate disintegration [9]. In this context, Campo *et* *al.* proved the improved AD of waste activated sludge (WAS) via thermo-alkaline digestate disintegration (4% NaOH at 70-90°C) with methane yields increased by 23% after digestate disintegration compared to an overall WAS pretreatment [13].

However, in digestate disintegration, the digestate age can affect the efficiency of the disintegration, as demonstrated by Cesaro et al. (2019) through ozonation (110 or 160 g O_3/ kg TS) of the organic fraction of municipal solid waste (OFMSW) digestate of different digestate ages (11 and 41 days old): the digestate of 41 days contained fewer accessible fractions compared to the digestate of 11 days corresponding to a higher COD solubilization in the 11 day old digestate than in the 41 day old digestate [14].

As alternative to the ozone treatment, the use of ultrasound for digestate disintegration was also investigated [9]. Ultrasound (US) applies cycling sound pressure waves (minimum frequency of 20 kHz) to create cavities in the liquid that cause mechanical shear forces upon implosion, thereby disintegrating the organic matter, decreasing its particle size and hydrolysing complex organic compounds into more soluble molecules [15]. As a consequence of the decreased particle size, the surface area increases and the hydrolytic rate of the microorganisms is enhanced [6]. Boni et al. demonstrated that US disintegration of organic waste and food waste digestate at a SE input of 50,000 kJ/kg TS, significantly increased the soluble total organic carbon (sTOC), soluble chemical oxygen demand (sCOD) and soluble carbohydrates (sCARB) by a 3.8-, and 14.4-fold, respectively, resulting in an increased biochemical methane potential (BMP) of 25% [12]. The same study moreover observed a linear correlation (R^2 ~ 0.9) between the solubilisation of dissolved organic matter (DOM) and the BMP of the disintegrated digestate, further validated by results of Somers *et al.* (2018).

It remains however unclear whether a causal relationship between COD solubilisation and BMP increase exists since lumped parameters such as COD or TOC do not provide adequate information about the structure of the digestate after disintegration in terms of bio-accessibility and complexity, hence leaving a gap in the in-depth knowledge of US-driven digestate disintegration. Unravelling the relationship between disintegration and bio-accessibility will enhance understanding of the literature on US digestate disintegrations and the efficiency of scenario 2 (Figure 1), and this has not previously been performed to the best of the authors' knowledge. A first challenge is to define the bio-accessibility, and this was addressed only in two studies. Jimenez *et al.* previously developed a method to characterize the bioaccessibility via chemical sequential extraction (CSE) of organic matter [3,4]. This method partitions the total COD of the organic matter in six different fractions, ranked from high to low bioaccessibility. Furthermore, the method utilizes 3D-excitation emission fluorescence spectroscopy to define the complexity ratio of the different organic fractions, based on their chemical composition. In this way, information regarding the structural changes that affect digestion efficiency and yield is gathered, providing a causal link between the effect of disintegrations and organic matter characteristics. Brémond *et al.* (2020) characterized untreated and treated solid agricultural digestates using the bioaccessibility method, and their results showed that the thermo-alkaline digestate treatment of solid agricultural digestate increased the bioaccessibility of the organic matter, which explained the 13% increase in methane yield [17].

The present study therefore aims to elucidate the effect of US on the structural organization of the organic matter in dairy manure digestate of two different digestate ages, and how these variables affect the methane yields during post-digestion (Scenario 2 in Fig. 1): if ultrasonication increases the bio-accessibility of digestate, it will lead to a higher methane yield during post-digestion, while simultaneously increasing the complexity of the DOM due to the formation of highly complex organic materials such as humic acid (HA)-like compounds. To the best of the authors knowledge, no publication so far discussed the effect of US digestate disintegration on the bioaccessibility and complexity of the organic matter. Such novel results are not found in the literature and will aid the development of the novel Scenario 2 post-digestion concept. For the purpose of this research, cow manure and its corresponding digestate (2 different digestate ages) were subjected to US disintegration and the resulting methane yield was assessed via BMP assays. The Jimenez *et al.* (2015) method was used to characterize and evaluate the bio-accessibility and complexity of the samples.

2. Materials and Methods

Two dairy manure digestates with a digestate age of respectively 29 and 43 days were disintegrated with ultrasound and fully characterized in terms of organic matter fractionation and BMP.

2.1 Manure and digestate samples

Dairy manure and dairy manure digestate were collected from a local dairy farm housing approx. 70 cows (Temse, Belgium). The digestate was collected from a mesophilic (37°C) farm-scale digester (140 m^3) which was fed daily with fresh dairy cow manure. The digester has a hydraulic retention time (HRT) of 25 days. Digestate samples were collected from the operations at the 25-day HRT and had hence an age of 25 days. The digestate samples were kept in jerrycans and stored in at a constant 37°C for 4 days until the experiments could start. This resulted in a simulated digestate age of 29 days, referred to as ‘Dig29’.

Simulation of extended digestate age

Dig29, was incubated in 1L lab-scale AD reactors, with a working volume of 0.8 L, purged with nitrogen gas and kept anaerobically at 37°C. The biogas production was monitored by water displacement. After 14 days, the digestate had a total age of 43 days and will thus be referred to as ‘Dig43’. The 14 days of digestion were considered to sufficiently decrease the VS content of the digestate, and thus comparison was considered meaningful since the extended digestion started from the same digestate composition.

2.2 Ultrasonication

The ultrasonication was carried out in a double-walled glass reactor with an active volume of 0.4 L. During ultrasonication, the digestate temperature kept at 25 °C by the water-cooled jacket, hence preventing thermal hydrolysis. The US reactor was stirred with an overhead stirrer (± 200 rpm) to ensure homogeneity. An HD3200 US generator with maximum power of 150 W (Bandelin, Berlin) was used to disintegrate the digestate samples. The US device consisted of a Sonopuls-497 US horn with a TT13 tip (both from Bandelin, Berlin). The tip was placed in the glass reactor at a liquid depth of approximately 3 cm. A power of 100 W and a frequency of 20 kHz were applied during the experiments, which resulted in a sonication density and intensity of 222 W/L and 113 W/cm², respectively. The specific energy (SE) was calculated according to equation (1).

$$SE = \frac{P*t}{V*TS} \qquad (1)$$

with P (W) as the US power, t (s) as the reaction time, V (L) as the volume and TS (%) being the total solid content. The specific energy was selected from previous research performed with a SE range of 3000 to 20003 kJ/kg TS. The lowest limit of this range was selected since research by Lippert *et al.* (2018), indicated that the highest energy recovery, i.e. the ratio of net regained energy production and the input US energy, was obtained by applying low SEs [18]. From the TS of the digestates, measured on the same day of the US and BMP experiments, and with a known US energy supply, the final SE was calculated to be 3029 kJ/kg TS and 2753 kJ/ Kg TS, with a respective average ultrasonication time of 15 and 12 minutes for Dig29 and Dig43.

2.3 Analysis of biochemical parameters

The soluble fractions were obtained in four steps: (i) centrifugation (10 minutes at 26,200 g), (ii) dilution of the supernatants, (iii) second centrifugation (10 minutes at 26,200 g) and (iv) filtration through a 0.6 µm filter paper. This four-step process prevents clogging of the filter paper and facilitates accurate soluble fraction measurements. After those steps, a secondary filtration through a 0.4 µm filter paper was performed to analyse the soluble chemical oxygen demand (sCOD). For all other soluble fraction measurements, i.e. total ammonia nitrogen (TAN) and the soluble organic nitrogen content, the 0.6 µm fraction was used. The amount of filtrate gathered from the 0.4µm filtration was insufficient to measure more than the sCOD, hence the 0.6 µm filtrate was used for these measurements.

Total solids (TS) and volatile solids (VS) were measured according to standard methods [19]. The pH was measured with a pH 3110 probe and the conductivity was measured by a graphite conductivity cell CDC-401 (both Hach Lange). The total chemical oxygen demand (tCOD) was measured after blending an approx. 400 mL sample for 1 minute at maximum power using a household blender (Bosch) and tCOD was analysed using Hach Lange test kits (LCK-014). TAN and soluble Kjeldahl nitrogen (sKJN) were measured using the Kjeldahl-method. After mineralization of the organic nitrogen (only for KJN) using the KjelFlex K-439 (Buchi, Flawil, Switzerland), the residual liquid was distilled (KjelFlex K-360, Buchi, Flawil, Switzerland). The distillate was subsequently titrated (Metrohm 848 Titrino plus) [20]. The soluble organic nitrogen (sOrgN) (in g N/L) was calculated according to equation (2).

$$sOrgN = sKJN - TAN \ [g \ N/L] \qquad (2)$$

The total volatile fatty acid (tVFA), expressed in mass acetic acid (HAc) per volume (g HAc/L), over total inorganic carbon (TIC), expressed in mass bicarbonate ions per volume (g HCO_3^-/L) ratio was determined using the Nordmann titration method with dilute sulfuric acid and was calculated by the empirical equations (3) and (4) [21]:

$$tVFA = \left[\left((Con\ B - Con\ A) * 20\ {}^{mL}/_{EF} * 1.66\right) - 0.15\right] * 500\ [mg\ acetate/L] \quad (3)$$

$$TIC = Con\ A * 250 * 20\ {}^{mL}/_{EF}\ [mg\ \ CaCO_3/L] \quad (4)$$

where ‘Con A’ is the volume (mL) of 0.1N H_2SO_4 used during the titration to pH 5.0. ‘Con B’ is the volume (mL) of 0.1 N H_2SO_4 during to titration from pH 5.0 to pH 4.4, and EF the sample volume (mL) which was approx. 5 mL.

The methane content of the biogas during digestion was measured by gas chromatography (GC) equipped with a thermal conductivity detector (TCD) operating at 110°C with a filament temperature at 210°C (TraceGC 1310, Thermo Scientific). The GC-column was a Molsieve 5A, 60-80, 3 meters (Agilent). The column temperature was maintained at 105 °C. Helium (99.999%, Air Liquide) was used as the carrier gas at a flow rate of 3 mL/min.

2.4 Chemical sequential extractions (CSE)

The CSE procedure links the biological accessibility of the digestate’s organic matter with its chemical accessibility, based on the mass balance of the obtained different fractions [4]. The solid matter obtained after centrifugation (10 minutes at 26,200 g) was subsequently freeze-dried at 0.2 mbar and -52°C and grinded using ball milling before the extraction procedure was carried out. After each extraction step, the reaction broth was centrifuged for 20 minutes at 18,600 g and 4°C. The COD of the filtrate was measured after 0.45 µm syringe filtration. The pellet formed after centrifugation was subsequently used in the next extraction step. The fraction definition of [5] was used: Dissolved Organic Matter (DOM), Soluble extractible fraction from Particular Extractable Organic Matter (SPOM), Readily Extractable Organic Matter (REOM), Slowly Extractable Organic Matter (SEOM), Poorly Extractable Organic Matter (PEOM) and Non-Extracted Organic Matter (NEOM) (Table 2).

Table 2: Extraction protocol and molecule fractions, arranged from high to low bio-accessibility. N is the number of the consecutive extraction steps to extract the respective fraction [4].

Fraction	Target molecules	N	Extraction protocol
DOM	soluble molecules	n.a.	sCOD
SPOM	Proteins, sugars	2	30 mL, 10 mM $CaCl_2$ for 15 min, at 30°C and shaking at 300 RPM
REOM	Proteins, nucleic acids, sugars, lipids	4	30 mL, 10 mM NaCl + 10 mM NaOH for 15 min, at 30°C and shaking 300 rpm
SEOM	Proteins, HA-like molecules, lipids	4	30 mL, N_2 flushed 0.1M NaOH for 60 min shaking at 300 rpm
PEOM	(hemi)cellulose	2	H_2SO_4 (25 mL, 72 % w/w), 1ste for 3 hours at 30°C and 300 RPM, and 2nd overnight at room temperature and no shaking
NEOM	Lignin-like molecules	n.a.	Non extracted COD, calculated from the mass balance

n.a.: not applicable

2.5 The use of 3D fluorescence spectroscopy

The extracts obtained during the CSE were analysed using fluorescence spectroscopy. The 3 Dimension Excitation Emission Matrix (3D-EEM) was plotted, using the excitation wavelength, the emission wavelength and corresponding emission intensity data gathered by Liquid Phase Fluorescence (EEM-LPF) [4]. The extracts obtained during the fractionation procedure were analysed on a LS55 Fluorescence analyser (Perkin Elmer).

The excitation wavelength was varied at 10 nm increments ranging from 200 to 600 nm, using a Xenon lamp emitting pulsed radiation (20 kW for 8 µs). The slit width was 10 nm for both excitation and emission beams. The fluorescence emission spectra were measured at a 90° angle from the excitation beam with a scan speed of 1200 nm/s. Hence, the fluorescence intensity was measured at every 0.5 nm. The obtained 3D EEM-LPF plot was decomposed in seven regions (I-VII) following Muller et al. (2014). These regions are based on the fluorescent properties of biochemical molecules (Table 3) [22,23].

Table 3: Respective excitation and emission wavelengths in nm, together with their detected typical molecules.

Region	Excitation (nm)	Emission (nm)	Molecules
I	<250	<330	Aromatic protein-like (tyrosine-like) materials
II	<250	330-400	Aromatic protein-like (thryptophan-like) materials
III	250 - 310	<400	Protein-like (tyrosine-like, thryptophan-like, microbial by-products)
IV	<260	>400	Fulvic acid-like materials
V	260-310	>400	Intern filter effect and glycated protein-like materials
VI	310-380		Glycolated protein-like (melanoidin) lignocellulose-like materials
VII	>380		Lipofuscin-like, lignine-like and humic acid-like materials

The region numbers of Table 3 were subsequently used to calculate the complexity ratio by equations (5) and (6) [22].

$$V_f(i) = \frac{V_{image}(i)}{COD_{extract}} * 1 \Big/ \frac{S(i)}{\sum_{i=I}^{VII} S(i)} \quad (5)$$

$$Complexity\ ratio = \frac{\sum_{i=IV}^{VII} V_f(i)}{\sum_{i=I}^{III} V_f(i)} \quad (6)$$

where $V_f(i)$ is the fluorescence volume per region (i) (U.A.nm²), V_{image} (U.A. g O_2/L) is the volume of the 3D plot, COD_{sample} is the COD (g O_2/L) of the extract, S(i) (nm²) is the area of the region (i).

The complexity ratio was defined as the ratio of the sums of the most complex fluorescence volumes (i.e. regions IV-VII) over the protein-like regions (I-III). In comparison with an extract of a higher complexity ratio, a lower complexity ratio hence corresponds to a higher concentration of easily biodegradable materials such as proteins and lower concentration of complex materials such as humic acids.

2.6 Biochemical methane potential assays

The biochemical methane potential (BMP) assays were conducted at mesophilic (37°C) conditions in 250 mL serum vials during approximately 49 days. The headspace was purged with nitrogen for approx. 15 seconds to ensure anaerobic conditions. The biogas production was measured with an acidified water displacement method [24]. The methane production was expressed at standard conditions (0°C and 1 atm) for dry biogas, using the online biogas app (OBA) tool for reference units [25]. Untreated digestate of the same digestate age (29 and 43 days, respectively) served as inoculum for the BMP assays since they were biochemically similar to the ultrasonicated digestates. A negative control, containing only the inoculum, was set up to determine residual methane production and was subtracted from the BMP results to obtain the net BMP of the VS added. A positive reference with cellulose as a substrate was added to verify the microbial activity of the inoculum. The BMP assays of the ultrasonicated digestates were conducted using a feed over microorganism (F:M) ratio in the range of 0.6-1.0 for Dig29 and Dig43, respectively. The differences in F:M ratio were a consequence of the differences in VS content. The BMP assays were conducted to assess: i) the additional methane production after ultrasonication and ii) the effect of US disintegration on digestate of different age. These BMP assays were labelled USDig29, USDig43, and Dig29, Dig43 for US treated and untreated digestate, respectively. In addition, the effect of US disintegration on the daily methane production rate (MPR) of the digestate was quantified by using a US disintegrated digestate without the addition of inoculum. These setups were labelled UX29 and UX43 for Dig29 and Dig43, respectively. These UX setups would evaluate the expected effect of inoculum on the bio-accessibility assessment after digestion. Lastly, BMP setups that are labelled as 'manure' were performed using Dig29 as inoculum and fresh manure as a substrate with an F:M ratio of 1.1. This allowed calculating the final methane yield after digestate post-digestion with and without US digestate disintegration. The BMP and MPR of the manure can furthermore be related to the bio-accessibility of the manure.

2.7 Statistical methods

All tests were run in triplicate, with the exception of the complexity analysis in which only two of the three repeat samples were analysed. A double-sided t-test was used to evaluate the statistical significance of the difference between two means. Statistical significance was established at the $p < 0.05$-level. Principal Component Analysis (PCA) was used for the interpretation of the data. PCA was performed in R© version 3.5.2 (2018-12-20) using package FactoMineR [26].

3. Results and discussion

Table 1 provides an overview of the digestate samples' biochemical parameters. The manure and digestates described in this table were further evaluated on their bioaccessibility and complexity.

Table 1: Biochemical parameters of the fresh manure and manure digestate samples of retention time 29 days (Dig29) and 43 days (Dig43), respectively.

Parameter	**Unit**	**Fresh Manure**	**Dig29**	**Dig43**
TS	%	8.3 ± 0.5	6.0 ± 0.1	5.8 ± 0.1
VS	%	6.2 ± 0.4	4.2 ± 0.1	3.9 ± 0.1
pH	-	7.3 ± 0.1	7.8 ± 0.1	7.9 ± 0.1
tCOD	g/L	93.6 ± 7.8	72.1 ± 4.6	53.9 ± 0.4
sCOD	g/L	14.8 ± 0.1	11.5 ± 0.1	12.2 ± 0.4
TAN	g N/L	1.5 ± 0.1	2.0 ± 0.1	2.1 ± 0.1
tKJN	g N/kg	4.1 ± 0.1	4.4 ± 0.1	4.2 ± 0.1
sKJN	g N/L	2.2 ± 0.2	2.7 ± 0.1	2.6 ± 0.0
tVFA	g HAc/L	6.2 ± 2.4	1.4 ± 0.5	3.0 ± 0.8
TIC	g HCO_3^-/L	9.5 ± 7.8	10.8 ± 5.4	12.2 ± 7.7
tVFA/TIC	g HAc/ g HCO_3^-	0.49 ± 0.34	0.08 ± 0.03	0.16 ± 0.06

3.1 Structural organization of organic matter

3.1.1 Manure digestion

Both raw dairy cow manure and its AD digestate were separately examined to make a comparison possible. The CSE of manure before and after digestion showed a significant decrease in organic matter, with 23% of the total COD and 32% of the VS having been degraded.

The digestion moreover considerably altered the bio-accessibility of the organic matter in the manure, especially towards its DOM and SPOM fractions that decreased during digestion by 24% and 62%, respectively (Fig. 2). The decrease in DOM was related to the microbial conversion of soluble COD to methane [2], while the decrease in the solid COD fractions (SPOM, REOM and PEOM) can be related to the hydrolysis of organic matter. The REOM fraction, mainly containing proteins, significantly decreased by 61% as a result of hydrolysis and subsequent conversion to biogas. The SEOM fraction, mainly containing humic acids and complex proteins, remained unaltered. This suggests that there was neither humic acid formation nor degradation. The PEOM fraction, containing mostly holocellulose, significantly decreased by 39% as a result of the hydrolysis and subsequent degradation. These findings were also supported by the PCA analysis. The data was decomposed into two principal components, called dimensions, which explained 88.15% of the total variance. The PCA showed a negative correlation between digestion time and the SPOM, SEOM, PEOM and NEOM mass fractions. This correlation further indicated that the bio-accessibility of organic matter decreased during digestion (Fig. 3). The extracts obtained during the CSE were analysed using fluorescence spectroscopy to obtain the complexity ratio. There were no significant changes in the complexity ratios of manure as a result of digestion, except for the REOM fraction, which was significantly increased by 34%. The complexity ratio of SPOM, SEOM and PEOM did increase, though not significantly. The removal of the proteins from the REOM fraction was indicated by the decrease in the fluorescence volume of regions I – III of the REOM extract, which caused an increased complexity ratio.

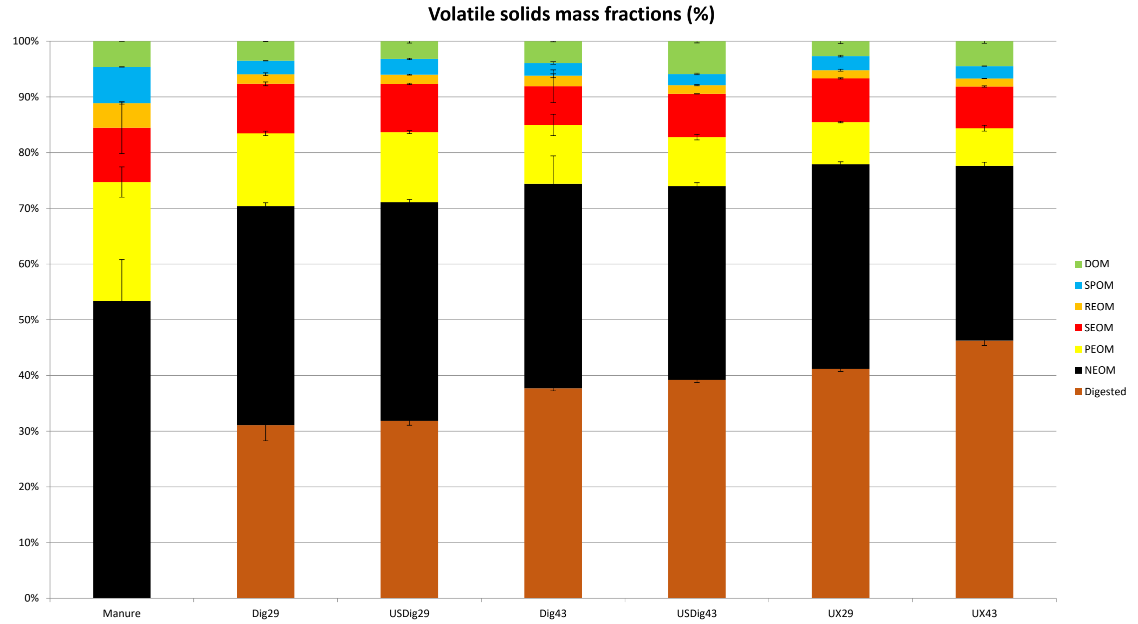

Figure 2: Mass fraction of the manure, the untreated and US treated digestate with digestate age of 29 days (Dig29 and USDig29, resp.), the untreated and US treated digestate with digestate age of 43 days (Dig43 and USDig43, resp.) and the US treated digestates after post-digestion (29 and 43 days) (UX29 and UX43, resp.).

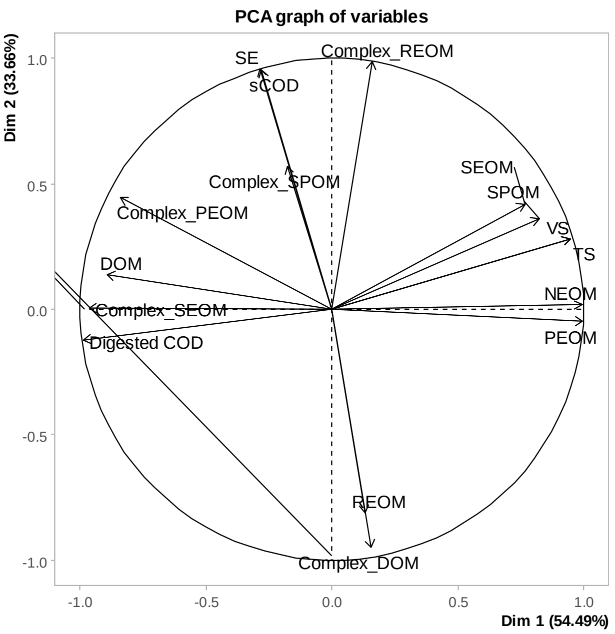

Figure 3: PCA mass fraction analysis, their respective complexity ratios, sCOD, and applied SE by ultrasonication

3.1.2 Influence of anaerobic post- digestion on the bio-accessibility and complexity

During the digestion of Dig29 for 14 days to reach Dig 43, 25% of the total COD and 7% of the VS were removed. However, no significant changes in the bio-accessibility of the digestates could be found due to the short digestion time of 14 days. The largest (albeit non-significant) decreases in bio-accessibility between Dig29 and Dig43 were in the fractions containing (i) the soluble particular proteins and sugars (SPOM, 6%), (ii) the slowly extractable proteins (SEOM, 22%) and (iii) the holocellulose fraction (PEOM, 19%). The 14-day post-digestion of Dig29 caused no significant changes in complexity, as shown in Fig. 4.

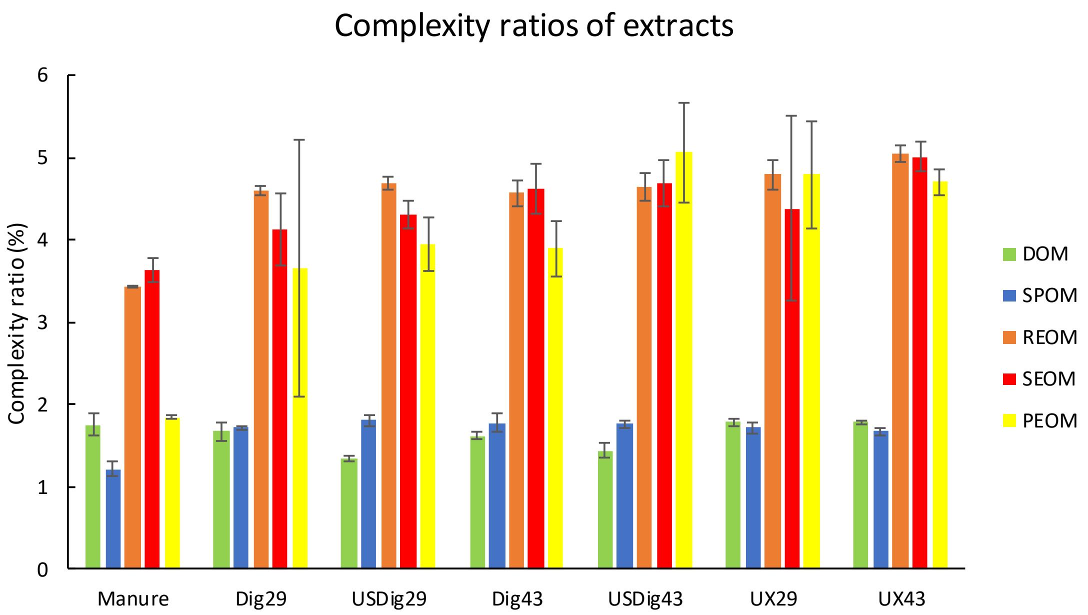

Figure 4: Complexity ratio, per mass fraction of raw manure, of the untreated and US treated digestate with 29 days of digestate age (Dig29 and USDig29, resp.), of the untreated and US

treated digestate of age 43 days (Dig43 and USDig43, resp.) and of the treated 29 and 43 days digestates after post-digestion (UX29 and UX43, resp.).

3.1.3 Effect of ultrasonication of bio-accessibility

Dig29 and Dig 43 were ultrasonicated with SEs of 2753 kJ/kg TS and 3029 kJ/kg TS, respectively. The TS value of the digestates was measured on the same day of the US disintegration, leading to small variations (< 10%) in the applied SE compared to the target SE of 3000 kJ/kg TS. Since the applied SE on Dig29 was lower compared to Dig43, while the relative sCOD release and BMP increase in Dig29 were higher compared to Dig43, the small deviations of the SE from the target SE can be neglected.

US disintegration increased the sCOD of Dig29 and Dig43 by 55% and 41%, respectively. This is also further supported by the PCA (Fig. 3). The increase in sCOD did not clearly translate into an increase in DOM due to the differences in centrifugation ratios. US disintegration of Dig29 released 28% more sCOD in comparison with Dig43. Compared with Dig43, Dig29 has relatively more organic materials in terms of VS and total COD present, that can be released by ultrasonication. Furthermore, the CSE before and after ultrasonication indicated a significant increase in the bio-accessibility as a result of solubilisation of easily degradable organic compounds of low complexity, such as proteins and carbohydrates. The SPOM fraction of Dig29 significantly increased by 17% due to ultrasonication. Conversely, the bio-accessibility of the solid fractions of Dig43 remained unaltered during ultrasonication. This indicated that in the digestate with the lower digestate age, ultrasonication repartitioned the COD from a less bioaccessible fraction to the SPOM fraction, which increased the accessibility of the soluble sugars and protein. However, in Dig43, there were less sugars and proteins present to enhance the bio-accessibility when compared with Dig29 and confirmed by the lower total COD (-25%) and VS content (-7%) of Dig43.

3.1.4 Ultrasonication can release particulate proteins

The extracts of Dig29 and Dig43 before and after ultrasonication were also analysed for the complexity ratio (Fig. 4). PCA revealed that the proteinaceous REOM fraction and the complexity of the DOM fraction were negatively correlated with the ultrasound SE, while the complexity of the SPOM and REOM fraction positively correlated with the SE (Fig. 3). This correlation was related to the ultrasound-induced repartitioning of low-complexity proteins from the SPOM and REOM fraction to the DOM fraction, thus confirming that there is no increase in DOM complexity due to US. The results indicating the solubilisation of proteins from the SPOM and REOM fraction were supported by the non-significant increase in the complexity of the SPOM and REOM fractions and the decrease in the complexity of the DOM fraction after ultrasonication. Meanwhile, the REOM mass fraction decreased non-significantly in both digestates after ultrasonication. Further support was obtained by measuring the soluble organic nitrogen in the DOM phase. Although the differences in soluble organic nitrogen concentration before and after ultrasonication could not be ascertained as significant due to the high standard deviations, the soluble organic nitrogen concentration increased by 21% and 16% for Dig29 and Dig43, respectively. Similar results were also found during the thermal treatment of sewage sludge. Zhang *et al.,* (2019) applied a similar CSE on thermally treated sewage sludge and observed the release of soluble protein to the DOM fraction which originated from the REOM and SEOM fractions [27]. Although the thermal treatment is considerably different from US, these findings further coincided with previous observations on the solubilisation of organically bounded proteins via US [28]. There were no significant effects measured on the TAN, FOS/TAC, pH, and the conductivity. These results can be found in the supplementary files.

3.2 Influence of the bio-accessibility on the anaerobic digestion yield and rate

3.2.1 BMP results

The BMP results of Table 4 show no statistically significant influence of the digestate age on the inoculum activity. However, ultrasonication of Dig29 significantly increased the BMP by 32% and 28%, respectively, with and without the inoculum addition. The addition of inoculum to USDig29 did not have a statistically significant effect on the BMP compared to UX29. The BMP of the manure was significantly higher than Dig29, which was a result of the higher bio-accessibility and higher biodegradability of the manure, compared to its digestate (Table 4).

On the other hand, ultrasound disintegration did not significantly increase the BMP of Dig43 (+35%, $p = 0.067$). As was the case with USDig29, there was also no significant difference in the BMPs of the USDig43 and UX43.

The differences in the BMP results of USDig43, compared to USDig29 were explained by the substrate bio-accessibility after US disintegration. As discussed above, US disintegration of Dig43 did not increase the bio-accessibility of its solid fractions. However, in the case of Dig29, the SPOM fraction was significantly increased after ultrasonication, which resulted in a more complete biodegradation of the organic matter and thus an increased the BMP of the US treated digestate. Furthermore, the BMP of Dig43 was 34% lower compared to Dig29, which indicated that Dig43 had more depleted organic matter. Furthermore, the additional methane yield gained by ultrasonication on Dig29 was not significantly different from the additional yield on Dig43.

This indicates that the difference in the BMP's after ultrasonication is only explained by the difference in digestate age.

Similar results were obtained by Cesaro et al., (2019), who reported that ozonation of OFMSW was indeed less efficient on a digestate with age of 41 days compared to 11 days in terms of increased COD solubilisation and biogas production after treatment [14]. A tentative energy balance is presented in the supplementary files. It has to be noted that the horn-type ultrasound inducer in to necessarily representative to an industrial set-up. Industrial set-ups can operate with a power higher than 100W used in this study. Higher powers result in greater disintegration efficiency compared to lower powers at equal SEs [15].

Table 4: BMP of the untreated digestates (Dig), the US treated digestate (USDig) and the US treated digestate without inoculum addition (UX) of Dig29 and Dig43.

BMP-values (mL CH_4/ g VS)	Dig29	Dig43
Positive reference	327 ± 29.8	282.7 ± 19.3
Dig	40.4 ± 0.2	26.0 ± 1.2
USDig	53.1 ± 2.0	35.0 ± 4.1
UX	51.8 ± 3.2	31.8 ± 2.5
Raw manure	152.9 ± 14.2	n.m.

n.m.: Not measured.

3.2.1 Methane production rates (MPR)

The MPRs of Dig29 and Dig43 are shown in Fig. 5, while the MPR of the positive reference and manure can be found in the supplementary files. The MPR of raw manure, during the first 30 days of the BMP assays, was significantly higher compared to Dig29 and Dig43, as a result of the higher bio-accessibility and lower complexity of the organic fractions of manure compared to Dig29 and Dig43.

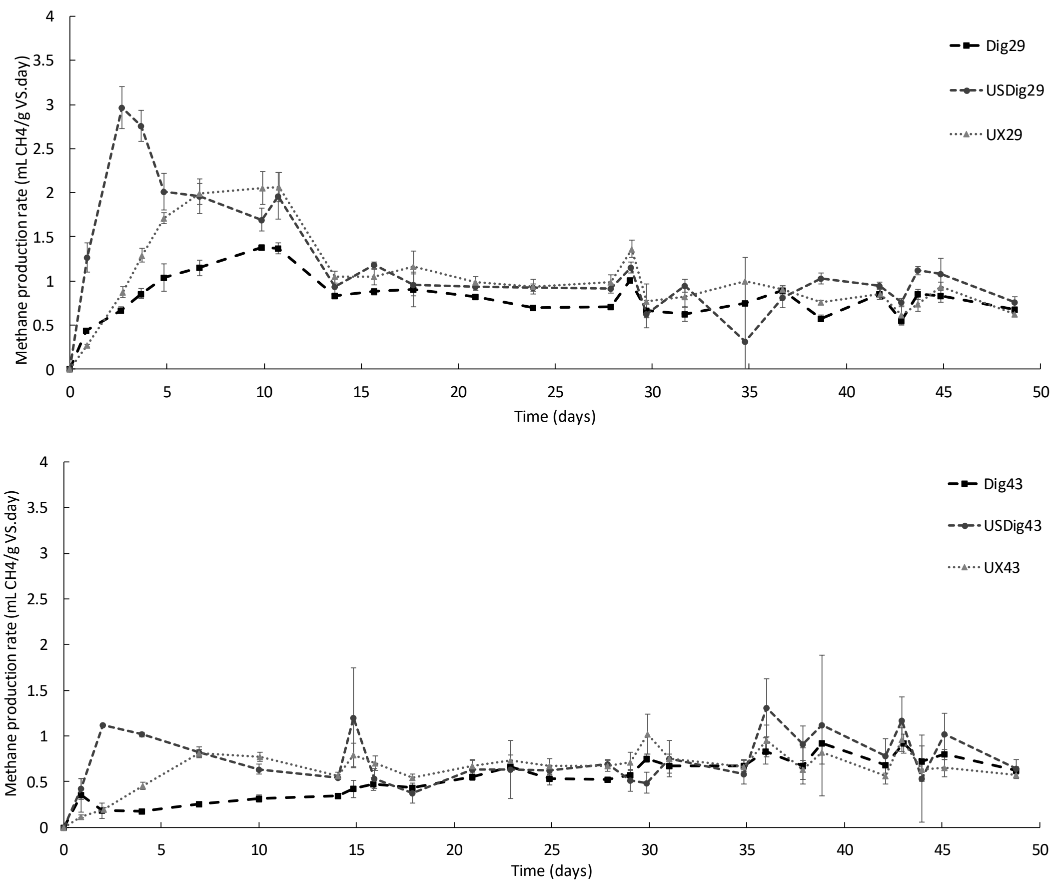

Figure 5: Daily methane production rates for the untreated digestates (Dig29 and Dig43), for the US treated digestates (USDig29 and USDig43) and for the BMP assays experiments without inoculum (UX29 and UX43).

Digestate disintegration improved the MPR during the first 5 days of digestion. The highest increase in the MPR was observed on the 3rd day of digestion with a 4.4-fold and a 6.2-fold increase for USDig29 and USDig43, respectively. The increased MPR was related to the significant increase in sCOD by 55% and 41%, after ultrasonication of Dig29 and Dig43, respectively. As the particulate proteins, carbohydrates and lipids were solubilised by ultrasonication, hydrolysis was increased which resulted in an increased MPR[15].

Moreover, when no inoculum was used during the post-digestion of the ultrasonicated digestate, the MPR did not increase to the same extent as inoculum added setups. The highest increase in MPR of UX29 and UX43 were a 1.7-fold and 3.2-fold of the Dig29 and Dig43 values respectively, both on the 7th day of digestion.

Between days 3 and 7 of digestion, the MPRs can be arranged in decreasing order as follows: USDig29 > UXDig29 > Dig29 and USDig43 > UXDig43 > Dig43 (Fig. 5). However, for both digestate ages, the MPR of the UX BMP-assay overtook the MPR of the US BMP-assay on the 7th day of digestion. The MPRs between day 7 and 11 were ordered as follows: UXDig29 > USDig29 > Dig29 and UXDig43 > USDig43 > Dig43. This pattern was replicated in a follow-up experiment in which dairy manure digestate with digestate age of 29 days was treated by US and consequently digested for 212 days. In this experiment, there was no significant increase in the BMP due to ultrasonication, however the increase in MPR was significant and the relative order of the MPRs with respect to digestate time, as described above, was also upheld. These results can be found in the supplementary information. The insignificant increases in BMP indicate that there was little to no organic material released by US, which would have otherwise not have been biodegradable by the microorganisms, given a sufficiently long digestion time. The observation that the increases in MPR of USDig29 and USDig43 were both higher and occurred sooner during the digestion, compared to the UX29 and UX43, indicated that the anaerobic microorganisms present in the digestates were, to some extent, negatively affected by ultrasonication by its disruption of the cell wall structures [29]. Clearly a correct balance between both the increased bio-accessibility and biodegradability of the disintegrated digestate, and the decreased activity of its microorganisms must be established prior to expanding the current BMP research results towards scaled-up continuous installations. The increased MPR’s found in this study indicate that post-digestion of ultrasonicated manure digestate can be done at lower HRT’s, or hence a smaller reactor volume or by higher mass flow rate.

4. Conclusions

Two digestates, i.e. Dig29 days and Dig43 days, were compared in terms of their changes in the biochemical parameter, bio-accessibility and complexity during US disintegration. The bioaccessibility of Dig29 was slightly increased as a result of the significant increase in the soluble particulate fraction of the proteins and carbohydrates. This resulted in an increase in the BMP of Dig29 by 32%. Although the bioaccessibility and BMP of Dig43 were not increased by ultrasonication, the daily methane production rates were increased in both ultrasonicated digestates. The differences in methane production rates between the different experiments in this study indicated that ultrasound negatively affected the microorganisms, but also that the extent of COD solubilisation outweighed those negative effects.

5. Acknowledgements

Matthijs H. Somers holds a Research Foundation – Flanders (FWO) Ph.D. fellowship (1S68017N). Parts of this research were conducted at INRAE-LBE (Narbonne) through a FWO travel grant (V404019N). The authors thank the INRAE-LBE researchers for their kind help and discussions during their research stay. Kris Heirbaut is acknowledged for providing the dairy cow manure and the dairy cow manure digestate.

6. References

[1] Maynaud G, Druilhe C, Daumoin M, Jimenez J, Patureau D, Torrijos M, et al. Characterisation of the biodegradability of post-treated digestates via the chemical accessibility and complexity of organic matter. Bioresour Technol 2017;231:65–74. https://doi.org/10.1016/j.biortech.2017.01.057.

[2] Appels L, Baeyens J, Degrève J, Dewil R. Principles and potential of the anaerobic digestion of waste-activated sludge. Prog Energy Combust Sci 2008;34:755–81. https://doi.org/10.1016/j.pecs.2008.06.002.

[3] Jimenez J, Gonidec E, Cacho Rivero JA, Latrille E, Vedrenne F, Steyer JP. Prediction of anaerobic biodegradability and bioaccessibility of municipal sludge by coupling sequential extractions with fluorescence spectroscopy: Towards ADM1 variables characterization. Water Res 2014;50:359–72. https://doi.org/10.1016/j.watres.2013.10.048.

[4] Jimenez J, Aemig Q, Doussiet N, Steyer JP, Houot S, Patureau D. A new organic matter fractionation methodology for organic wastes: Bioaccessibility and complexity characterization for treatment optimization. Bioresour Technol 2015;194:344–53. https://doi.org/10.1016/j.biortech.2015.07.037.

[5] Jimenez J, Lei H, Steyer JP, Houot S, Patureau D. Methane production and fertilizing value of organic waste: Organic matter characterization for a better prediction of valorization pathways. Bioresour Technol 2017;241:1012–21. https://doi.org/10.1016/j.biortech.2017.05.176.

[6] Azman S, Khadem AF, Van Lier JB, Zeeman G, Plugge CM. Presence and role of anaerobic hydrolytic microbes in conversion of lignocellulosic biomass for biogas

production. Crit Rev Environ Sci Technol 2015;45:2523–64. https://doi.org/10.1080/10643389.2015.1053727.

[7] Baeyens J, Appels L, Peng L, Dewil R. The production of bio-energy by microbial (biogas through anaerobic digestion) or thermal (pyrolysis) processes. Renew Energy 2016;96:1055. https://doi.org/10.1016/j.renene.2016.06.012.

[8] Ferreira LC, Souza TSO, Fdz-Polanco F, P??rez-Elvira SI. Thermal steam explosion pretreatment to enhance anaerobic biodegradability of the solid fraction of pig manure. Bioresour Technol 2014;152:393–8. https://doi.org/10.1016/j.biortech.2013.11.050.

[9] Garoma T, Pappaterra D. An investigation of ultrasound effect on digestate solubilization and methane yield. Waste Manag 2018;71:728–33. https://doi.org/10.1016/j.wasman.2017.03.021.

[10] Lindner J, Zielonka S, Oechsner H, Lemmer A. Effects of mechanical treatment of digestate after anaerobic digestion on the degree of degradation. Bioresour Technol 2015;178:194–200. https://doi.org/10.1016/j.biortech.2014.09.117.

[11] Dewil R, Appels L, Baeyens J, Degrève J. Peroxidation enhances the biogas production in the anaerobic digestion of biosolids. J Hazard Mater 2007;146:577–81. https://doi.org/10.1016/j.jhazmat.2007.04.059.

[12] Boni MR, D'Amato E, Polettini A, Pomi R, Rossi A. Effect of ultrasonication on anaerobic degradability of solid waste digestate. Waste Manag 2016;48:209–17. https://doi.org/10.1016/j.wasman.2015.10.031.

[13] Campo G, Cerutti A, Zanetti M, Scibilia G, Lorenzi E, Ruffino B. Enhancement of waste activated sludge (WAS) anaerobic digestion by means of pre- and intermediate treatments. Technical and economic analysis at a full-scale WWTP. J Environ Manage

2018;216:372–82. https://doi.org/10.1016/j.jenvman.2017.05.025.

[14] Cesaro A, Belgiorno V, Siciliano A, Guida M. The sustainable recovery of the organic fraction of municipal solid waste by integrated ozonation and anaerobic digestion. Resour Conserv Recycl 2019;141:390–7. https://doi.org/10.1016/j.resconrec.2018.10.034.

[15] Tyagi VK, Lo S-L, Appels L, Dewil R. Ultrasonic treatment of waste sludge: A review on mechanisms and applications. Crit Rev Environ Sci Technol 2014;44:1220–88. https://doi.org/10.1080/10643389.2013.763587.

[16] Somers MH, Azman S, Sigurnjak I, Ghyselbrecht K, Meers E, Meesschaert B, et al. Effect of digestate disintegration on anaerobic digestion of organic waste. Bioresour Technol 2018;268:568–76. https://doi.org/10.1016/j.biortech.2018.08.036.

[17] Brémond U, Bertrandias A, Loisel D, Jimenez J, Steyer JP, Bernet N, et al. Assessment of fungal and thermo-alkaline post-treatments of solid digestate in a recirculation scheme to increase flexibility in feedstocks supply management of biogas plants. Renew Energy 2020;149:641–51. https://doi.org/10.1016/j.renene.2019.12.062.

[18] Lippert T, Bandelin J, Musch A, Drewes JE, Koch K. Energy-positive sewage sludge pre-treatment with a novel ultrasonic flatbed reactor at low energy input. Bioresour Technol 2018;264:298–305. https://doi.org/10.1016/j.biortech.2018.05.073.

[19] APHA. Standard Methods for the Examination of Water and Wastewater. Stand Methods 2005:541. https://doi.org/ISBN 9780875532356.

[20] Sambusiti C, Monlau F, Ficara E, Musatti A, Rollini M, Barakat A, et al. Comparison of various post-treatments for recovering methane from agricultural digestate. Fuel Process Technol 2015;137:359–65. https://doi.org/10.1016/j.fuproc.2015.04.028.

[21] Kafle GK, Kim SH. Sludge exchange process on two serial CSTRs anaerobic digestions: Process failure and recovery. Bioresour Technol 2011;102:6815–22. https://doi.org/10.1016/j.biortech.2011.04.013.

[22] Muller M, Jimenez J, Antonini M, Dudal Y, Latrille E, Vedrenne F, et al. Combining chemical sequential extractions with 3D fluorescence spectroscopy to characterize sludge organic matter. Waste Manag 2014;34:2572–80. https://doi.org/10.1016/j.wasman.2014.07.028.

[23] Chen W, Westerhoff P, Leenheer JA, Booksh K. Fluorescence Excitation-Emission Matrix Regional Integration to Quantify Spectra for Dissolved Organic Matter. Environ Sci Technol 2003;37:5701–10. https://doi.org/10.1021/es034354c.

[24] Wang B, Nges IA, Nistor M, Liu J. Determination of methane yield of cellulose using different experimental setups. Water Sci Technol 2014;70:599–604. https://doi.org/10.2166/wst.2014.275.

[25] Hafner SD, Rennuit C, b. Getting started with the biogas package. Https://BiotransformersShinyappsIo/Oba1/ 2018.

[26] Lê S, Josse J, Husson F. FactoMineR: An R Package for Multivariate Analysis. J Stat Softw 2008;25:1–18. https://doi.org/10.1016/j.envint.2008.06.007.

[27] Zhang Y, Xu S, Cui M, Wong JWC. Effects of different thermal pretreatments on the biodegradability and bioaccessibility of sewage sludge. Waste Manag 2019;94:68–76. https://doi.org/10.1016/j.wasman.2019.05.047.

[28] Elbeshbishy E, Aldin S, Hafez H, Nakhla G, Ray M. Impact of ultrasonication of hog manure on anaerobic digestability. Ultrason Sonochem 2011;18:164–71. https://doi.org/10.1016/j.ultsonch.2010.04.011.

[29] Pilli S, Bhunia P, Yan S, LeBlanc RJ, Tyagi RD, Surampalli RY. Ultrasonic pretreatment of sludge: A review. Ultrason Sonochem 2011;18:1–18. https://doi.org/10.1016/j.ultsonch.2010.02.014.